NASA Technical Memorandum 103135
AIAA–90–1994

Digital Filtering of Plume Emission Spectra

George C. Madzsar
Lewis Research Center
Cleveland, Ohio

NASA

DIGITAL FILTERING OF PLUME EMISSION SPECTRA

George C. Madzsar
National Aeronautics and Space Administration
Lewis Research Center
Cleveland, Ohio 44135

Abstract

Fourier transformation and digital filtering techniques were used to separate the superpositioned spectral phenomena observed in the exhaust plumes of liquid propellant rocket engines. Space shuttle main engine (SSME) spectral data were used to show that extraction of spectral lines in the spatial frequency domain does not introduce error, and extraction of the background continuum introduces only minimal error. Error introduced during band extraction could not be quantified due to poor spectrometer resolution. Based on the atomic and molecular species found in the SSME plume, it was determined that spectrometer resolution must be 0.03 nm for SSME plume spectral monitoring.

Introduction

Spectral analysis of the radiation emitted from the exhaust plume of an oxygen - hydrogen (OH) fueled rocket engine reveals the constituents[1-5] and the state(s)[6-8] of the exhaust gases. Engine health and performance characteristics can be inferred from knowledge of the exhaust constituents and states.

An inherent assumption with plume spectral analysis is that the spectral characteristic(s) identifying a particular constituent or state can be distinguished from all other spectral phenomena occurring simultaneously within the plume. This assumption is not always correct. A high resolution spectrometer can separate closely spaced spectral lines, however, it cannot separate superpositioned spectral phenomena. Since the overall irradiance from a plume is the sum of irradiances from numerous discrete spectral sources, superpositioning does occur, thereby preventing direct determination of the absolute irradiances from discrete spectral phenomena.

This paper demonstrates the application of Fourier and digital filtering techniques to the analysis of rocket engine plume spectra. These tools offer the capability to dissect a spectrum and examine its specific features in detail.

Background

By monitoring the contents of the rocket engine exhaust, it is possible to determine which material(s), and therefore which components within the engine, are eroding. Figure 1 displays the propellant flow paths of the space shuttle main engine (SSME). All particulates eroding from internal engine components within the flow path end up in the combustion chamber where they burn and exit through the exhaust nozzle. Knowledge about the state of the exhaust gases is beneficial for evaluation of the combustion process. Spectral emissions from the by-products of OH based combustion can provide information about propellant mixture ratio, and the blackbody radiation from particulates can provide information about the temperature in the combustion chamber.

Table 1 is a partial list of SSME materials and their corresponding emission wavelengths. The wavelength values are based on past SSME firings,[1] and predicted values.[9,10] As of this writing, the spectral phenomena of interest lie between the far ultraviolet and near infrared wavelengths. Observing spectral irradiance at wavelengths which correspond to engine structural materials as a function of time identifies both the species and relative rates of material erosion. Based upon the state of the exhaust gases and the species and rate of the material erosion, relative health and performance of the rocket engine can be determined.

Figures 2 to 4 display typical emission spectra from the SSME. As evident from Fig. 2, line emissions are superimposed on band emissions, which are superimposed on a background continuum. A series of emission spectra recorded as a function of time from an SSME are displayed in Fig. 3. The x, y and z axes correspond to wavelength, irradiance, and time respectively. The initial spectrum was recorded just after engine ignition, and subsequent spectra were recorded at 0.1 sec intervals. As can be seen, irradiance levels change substantially over time.

The current technique used to analyze SSME spectral data consists of tracking irradiance levels at wavelengths corresponding to specific engine materials, without considering the effects of spectral superpositioning.[1-4] This method is acceptable if a proportionality constant between the irradiances of the various spectral phenomena exists, and does not change with engine operating conditions. This proportionality constant is dependent on the amount and species of impurities in the propellants, the rate of material erosion from engine components, propellant mixture ratio, combustion chamber pressure and temperature, and propellant flow rates. From the spectral diversity seen in Figs. 2 to 4, it may be difficult to determine if a proportionality constant even exists. In Fig. 3, the continuum and spectral line irradiances vary with respect to time (corresponding to power level changes), and vary with respect to each other. In Fig. 1, spectral line and continuum irradiances appear substantially different than the corresponding irradiances seen in Figs. 2 and 3. Considering these variations, it could not, for example, be determined if a change in the irradiance at a wavelength corresponding to a metal is due to a change in the rate of metal erosion, due to a change in the continuum onto which the metallic spectral line is superimposed, or due to changes in both the continuum and the rate of metal erosion. Using simple background subtraction to isolate background changes from line changes is not ideal since with background subtraction, absolute irradiance of the spectral line may be lost. Also, background subtraction cannot separate line from band emissions.

Note that the spectra displayed in Figs. 2 to 4 were selected to demonstrate the diversity of SSME plume emissions. From these figures, the following inferences can be made: First, it may be difficult

to establish a baseline spectral signature due to gross differences in the spectra from different engines. Second, the use of narrow band pass optic filters to view a few specific wavelengths without regard to irradiances at neighboring wavelengths is precluded.

Theory

To relate Fourier and digital filtering techniques to plume spectral analysis, consideration must be given to the physics of spectral emissions, and the mathematics of Fourier analysis. The interactions between the sources of plume emissions, causes for variations in plume emissions, Fourier theory, filter implementation, and errors associated with digital filtering need to be understood. Following is a discussion on these issues.

Spectral radiation is the result of photon emission during the combustion of propellants, the burning of impurities in the propellants, and the burning of materials that may have eroded from internal engine components. Energy released during the combustion process excites the atomic, molecular and chemical species within the combustion chamber, which in turn, emit photons. Photon wavelength(s) are a characteristic of their source. Potential types of emissions and sources of photons include the following:[11,12]

(1) Line emission from atomic transitions due to thermal excitation.

(2) Line emission from atomic transitions excited by chemical reactions.

(3) Band emission from thermally excited molecules.

(4) Band emission from chemically excited molecules.

(5) Continuum radiation from chemical reactions.

(6) Continuum blackbody radiation from particulates.

Line and bandwidths of these emissions are as their names imply; line emission appears as narrow spectral lines, band emission consists of spectral emissions distributed over a finite band of wavelengths, and the continuum covers the entire spectrum in the observed wavelength range.

In optically thin gases, the shapes of the spectral lines are determined primarily by the velocity and collisional behavior of the emitting species. Factors contributing to variations in the lineshape include the following:[11]

(1) Doppler broadening - due to relative motion between atoms and the observer.

(2) Field broadening - result of electrical (Stark effect) or magnetic (Zeeman effect) fields.

(3) Holtsmark broadening - result of collisions between like atoms.

(4) Lorentz broadening - results from the collision of unlike atoms.

(5) Natural broadening - linked to the radiative lifetime through the Heisenberg uncertainty principle.

In an OH rocket engine plume, the population of metallic species is relatively small compared to the population of combustion species, resulting in minimal Holtsmark broadening of metallic lines. Field broadening is minimal since external magnetic and/or electric fields are not applied. Natural linewidths of atomic emission are on the order of 10^{-6} nm and the Lorentz and Doppler linewidths are on the order of 10^{-3} nm. Therefore, only Doppler and Lorentz broadening need to be considered for line emissions. Broadening does not need to be considered for the continuum and band emissions since broadening induced width variations are small when compared with the natural widths of these phenomena. These differences in line/band widths are the key feature that enable Fourier techniques to separate spectral phenomena.

Fourier techniques enable separation of spectral phenomena since different types of spectral emissions have different bandwidths, and therefore different spatial frequencies. The continuum, with a bandwidth covering the entire spectrum, has a relatively low spatial frequency. Line emissions have high spatial frequencies, and band emissions have spatial frequency components greater than that of the continuum, and less than that of the lines.

The Fourier transform is a mathematical tool that relates time or space domain data to its corresponding frequency (or spatial frequency) representation.[13-16] The Fast Fourier Transform (FFT) is an efficient computer implementation of the Fourier transform. With respect to spectroscopy, the space domain of a spectrum is transformed into its spatial frequency counterpart. For spectroscopic applications, the aspects of Fourier theory that must be considered are the spatial sampling interval, issues of data nonperiodicity, and the number of spectral data points to be transformed.

The spatial sampling interval is defined as dx, where dx is the resolution of the spectrometer. The Nyquist limit, defined as 1/(2 dx), is the greatest frequency that can be resolved without aliasing errors being introduced into the data set. Therefore, an emission spectrum with sampled data is bandwidth limited to spatial frequencies less than or equal to one-half of the spatial sampling rate. With respect to spectroscopy, two factors must be considered when determining the required spatial sampling rate. The spatial sampling rate must be adequate to resolve closely spaced spectral lines, and adequate to enable separation of the line, band and continuum spatial frequency components.

A potential error in Fourier transformed data can be caused by the nonperiodicity of the data set that is being transformed, and the assumption that the total duration of the response is the same as the period of the data set.[14] If a data stream is nonperiodic (as are plume spectra), the periodicity assumptions will result in "pollution" of the transformed data set at its two ends. This wraparound characteristic, which is inherent to the FFT, may be overcome by creating a buffer zone containing zeroes at the two ends of the data stream prior to transformation. The number of padding values added at each end of the data stream is equal to half of

2

the total number of data points in the unpadded
set. The resultant padded set contains twice the
number of data points as in the original unpadded
data set, while maintaining the power of two data
points that are required for the FFT.

If the data set is offset, that is the first
and last values of the data set are not equal to
zero, zero padding will introduce vertical edges.
Vertical edges will exhibit the characteristic
sin(x)/x, or damped "ringing" at frequencies corre-
sponding to the edges when the data set is trans-
formed. This may be avoided by subtracting the
values of the straight line connecting the first
and last points from the entire data set, and then
padding with zeroes. However, the absolute irradi-
ance levels of the original data will then be lost.
An alternate method is to pad the left side of the
data set with the value of the first data point of
the original unpadded set, and to pad the right side
of the data set with the value of the last data
point of the original unpadded set.

Filtering in the frequency domain is performed
by removing the spatial frequency components corre-
sponding to unwanted spectral phenomena. For fil-
tering, the spectrum is sampled, digitized, padded,
and transformed into its frequency representation.
The transformed data is multiplied by a filter func-
tion which removes all unwanted spatial frequency
components. The resultant data is transformed back
into its original domain via the inverse FFT. A low
pass filter extracts the spatial frequency compo-
nents of the continuum, a band pass filter extracts
the components of the band emissions, and a high
pass filter extracts the components of the line
emissions. Key issues with this method of filter-
ing are the filter cutoff spatial frequencies, and
the filter function shape.

The cutoff spatial frequency defines the bound-
ary between the filtered and unfiltered regimes on
the transformed spectrum. This cutoff can be deter-
mined analytically from the theoretical widths of
spectral phenomena. Line emissions have widths on
the order of 10^{-3} nm after broadening. Since
spatial frequency is defined as 1/bandwidth, line
emissions have spatial frequencies on the order of
1000 cycles/nm. Band emissions typically have band-
widths on the order of 10 nm, corresponding to
spatial frequencies of 0.1 cycles/nm. Setting the
cutoff spatial frequency of the filter between these
values will separate them.

The rising and/or falling edges of the filter
cutoff should not be vertical, since these edges
will be transferred to the data set upon application
of the filter. Upon inverse transformation, any
vertical edge will appear as a sin(x)/x function in
the filtered spectrum. A Gaussian, sine or cosine
function may be used to develop the rising and fall-
ing edges of the filter.

Note that individual classes of emissions
(line, band, continuum) contain spatial frequency
components in the other classes, since spectral
emissions typically cannot be expressed as a per-
fect sinusoidal waveform of a single spatial fre-
quency. Therefore, filtering for a specific class
of emissions introduces errors. This error is rela-
tively small if the magnitudes of the spatial fre-
quency components outside of its class are small,
and can be minimized by careful selection of cutoff
spatial frequencies.

Experimental Implementation

Plume emission spectra can be measured with
equipment similar to that shown in Fig. 5. Radia-
tion emitted from the shock diamond within the
plume is focused onto a bundle of optical fibers,
which transmit the light to a spectrometer. The
shock diamond serves as the focal point since plume
irradiance is greatest at that location. Optical
fibers are used since they enable the delicate spec-
trometer to be placed away from the harsh engine
environment. The spectrometer separates the light
into its constituent wavelengths. This spectrum is
imaged onto a linear photo diode array, which meas-
ures the irradiance as a function of wavelength.
All plume spectra displayed in this paper were
recorded at the NASA Stennis Space Center from an
SSME during test firing.

The spectra shown in this paper were measured
with a 256 element diode array on a 0.5 m focal
length spectrometer, with a nonrotating 300 groves
per millimeter grating. This arrangement yields a
wavelength range of 300 to 825 nm, a resolution of
$(825-300)/256 \approx 2.1$ nm, and a Nyquist limit of
0.25 cycles/nm. The resolution, limited primarily
by the diode array density, is poor, and does not
allow for accurate measurements of closely spaced
or narrow spectral lines. With the Stennis equip-
ment, two complete spectral scans per second can be
measured, digitized and transferred to a storage
medium.

Figure 6 displays the spectrum from Fig. 4
after transformation, along with superimposed high,
low and band pass filter functions. The upper spa-
tial frequency in Fig. 6 corresponds to the Nyquist
limit. Note that the magnitude of the transformed
spectrum is plotted in a logarithmic scale to graph-
ically emphasize small changes, and the filter func-
tions are plotted in a dimensionless absolute linear
scale extending from 0.0 to 1.0.

Selection of cutoff frequencies for the vari-
ous filters was not simple due to poor spectrometer
resolution. The spectrometer, with a resolution of
2.13 nm, measured irradiances of spectral lines with
widths of 10^{-3} nm. This resulted in measured line
widths of the same order-of-magnitude as the actual
widths of the bands. Upon transformation, line and
band spatial frequency components overlapped.
Therefore, the cutoff frequencies were determined
by trial and error. The cutoff frequencies were as
follows: 0.025 cycles/nm for the low pass filter,
0.025 cycles/nm for the high pass filter, and 0.010
through 0.210 cycles/nm for the band pass filter.

Results

The results of low pass, high pass, and band
pass filtering can be seen in Figs. 7 to 9 respec-
tively. In Fig. 7, two curves are displayed. The
dotted line is the unfiltered spectrum, and the
solid line is the spectrum after low pass filtering.
Figures 8 and 9 display the filtered spectrum along
with the noise floor. Analysis indicated that low
and high pass filtering introduce only minimal
error. Band pass filtering does not clearly indi-
cate the capability to extract band emissions. It
was concluded that poor spectrometer resolution
caused this problem. Poor resolution also caused
difficulties with the separation of closely spaced
spectral lines. Electrical and/or optical noise
was relatively low, indicating a high signal to

3

noise ratio. Following is a detailed discussion of these results.

By comparing the unfiltered to the low pass filtered spectrum in Fig. 7, it can be seen that the higher spatial frequency line and band components were removed, as expected. Also from Fig. 7 the reasonableness of the low pass filter can readily be seen, since the filtered spectrum is clearly a smooth fit to the unfiltered spectrum.

The continuum and most lower spatial frequency band emissions were removed by the high pass filter, as seen in Fig. 8. To check the validity of the filtered spectra, irradiance of the sodium line at 589 nm was examined. First, sodium irradiance was determined by subtracting the low pass filtered spectra from the unfiltered spectra. The irradiance value at 589 nm from this subtraction was compared with that from the high pass filtered spectra. The difference between these values was approximately 8 percent, indicating good correlation. In Fig. 8 some lines have multiple species identification labels on them. This resulted from poor spectrometer resolution, which did not enable resolution of closely spaced lines.

It is evident from Fig. 8 that irradiances after filtering can be extremely small, raising concerns with the signal to noise ratio. Typically, system noise is determined from the dark current that is measured by the individual diodes, and signal to noise is determined by comparing the dark current values to the spectral irradiance values. For this paper the actual signal to noise ratio could not be determined since the dark current scans were not available from Stennis. To perform noise analysis, the dark current value as specified by the diode manufacturer was used. These specifications stated that the maximum dark current noise for any diode is 1 percent of the saturated signal. Therefore, assuming that the peak measured irradiances are near the saturation point, the maximum noise level can be determined. The dashed line in Fig. 8 indicates this 1 percent noise floor.

With Fourier analysis, averaging improves the signal to noise ratio. For emission spectroscopy however, averaging prevents observation of sudden irradiance changes indicative of engine degradation. For spectroscopic applications, signal to noise is optimized through selection of the diode integration time. The integration time must be long enough to insure that the measured irradiances are substantially above the detector dark current, yet short enough to prevent diode saturation, and short enough to enable processing of sudden irradiance changes. The overall irradiance from the SSME plume is sufficiently large so long integration times are not required.

Interesting observations can be made from the extracted phenomena seen in Fig. 8. First, the majority of lines observed in Fig. 8 can be identified from Table 1. Second, noise does not appear to be a problem. Third, it is evident that a great deal of spectral activity is occurring within the plume. The lines corresponding to sodium and potassium are clearly visible. These elements are introduced as impurities in the propellants. Excluding these lines, it is evident that many structural elements are burning. The chromium, copper, iron, nickel, and cobalt lines are present, indicating material erosion. Lithium and calcium lines are present, indicating bearing wear. Typically, all components within the flow path of the engine erode to some degree. However, a sudden change in the amount of erosion could indicate accelerated erosion and/or impending component failure.

Figure 9 displays the spectrum shown in Fig. 4 after band pass filtering, with the dashed line indicating the 1 percent noise floor. As can be seen, band emissions are not accurately extracted. While some bands can be identified, it appears that many unknown artifacts are present. This was due to a number of reasons. First, band emissions were not prominent in the unfiltered spectrum, as evident from Table 1 and Fig. 4. Second, poor spectrometer resolution did not enable separation of the line and band spatial frequency components. And third, some spatial frequency components of the bands were lost during filtering. It appears that the second and third causes are the predominant drivers in the inability to extract band emissions.

Poor spectrometer resolution causes line emissions to appear much broader than they actually are. A resolution of 2.1 nm implies that the measured wing of a line is at least 2.1 nm wide, and that the narrowest measurable line width is 4.2 nm. This causes difficulties with spatial frequency overlap, since widths of the artificially broadened lines as measured by a spectrometer are in the same order-of-magnitude as the actual widths of the bands. This overlap precludes the formation of a distinct boundary between the frequency components of the lines and bands. With no distinct boundary, a cut off spatial frequency for the filter cannot be determined.

Since Fourier transformation converts the spectra into a series of sinusoidal components, the decomposition of a specific type of spectral emission will typically be expressed over a range of spatial frequencies rather than at a single spatial frequency. This could translate into a specific type of emissions (line, band, and continuum) having sine components over a broad range of spatial frequencies, some of which may overlap with the sine components of the other types of emissions. If the magnitudes of the overlapping components from one type of emission are large with respect to the magnitudes of the other type of emission, filtering will corrupt the data.

From Fig. 4 and 7 it can be seen that line emissions occur at high spatial frequencies only. Therefore, removing the lower spatial frequency components with a high pass filter does not introduce error. While the continuum consists mainly of low spatial frequency components, it may have some components at the higher frequencies, which will be filtered out by a low pass filter. From Fig. 5 it can be seen that magnitudes at the low spatial frequencies are substantially greater than magnitudes at all other spatial frequencies, indicating that higher frequency components of the continuum are negligible. Therefore, low pass filtering introduces only minimal error. The magnitudes at spatial frequencies corresponding to the band emissions are relatively small, but could not be distinguished from continuum and line frequency components. Since the bands could not be accurately extracted, errors associated with this process could not be quantified.

A conclusion from the preceding discussion is that line versus band characteristics drive the spectrometer resolution requirements. However, the resolution of the spectrometer must be adequate to separate closely spaced lines as well as separate the line/band spatial frequencies. From Table 1, nearest lines from different metallic species are the copper line at 353.04 nm, and the cobalt line at 352.98 nm. Assuming these are the nearest lines that must be resolved, the required resolution can be determined. The numeric difference between these lines is 0.06 nm. With respect to the Nyquist criteria, the spectrometer must therefore be capable of resolving 0.03 nm to separate these lines. With this resolution, the measured line widths will be greater than the actual line widths after broadening, indicating that broadening induced line overlap will not be of concern. This resolution corresponds to a spatial frequency of 33.33 cycles/nm, which is two orders-of-magnitude greater than the spatial frequencies of the band emissions. Therefore, this resolution is sufficient to separate lines and bands, as well as resolve closely spaced lines.

The spectrum shown in Fig. 4 was recorded from engine number 2031 during firing number 904-047, on August 11, 1989. This particular spectrum corresponds to emissions occurring 3 sec after engine ignition. Analysis of the 100 sequential scans recorded during the first 50 sec of firing time from this engine using the techniques discussed in this paper revealed no anomalous engine behavior or accelerated material erosion. Viewing the unfiltered emission spectra as a function of time did reveal changing irradiance levels. However, upon filtering, irradiances of the spectral lines corresponding to metallic species were constant with respect to engine power level, indicating normal engine wear. The same conclusion was reached during post firing analysis of the engine.

Conclusions

Fourier and digital filtering techniques enable separation and extraction of superpositioned spectral phenomena observed in the plumes of OH fueled rocket engines. Fourier transformation separates spectral phenomena as a function of spatial frequency, and filtering in the spatial frequency domain extracts the specific spectral phenomena.

In the spatial frequency domain, spectral line emissions appear as the high spatial frequency components, the continuum appears as the low spatial frequency components, and the band emissions appear at spatial frequencies between the line and continuum components. A high pass filter extracts the line emissions, a low pass filter extracts the continuum, and a band pass filter extracts the band emissions. Cutoff frequencies for the filter functions can be estimated analytically from the theoretical widths of the various spectral phenomena. To utilize these theoretical cutoff values, resolution of the spectrometer must be adequate to enable resolution of the spatial frequencies in the range of the calculated cutoff values.

High pass filtering does not introduce error since line emissions consist of high spatial frequency components only. Low pass filtering introduces minimal error since the continuum contains some low magnitude higher spatial frequency components which are filtered out. Error introduced by band pass filtering could not be quantified, since

band emissions contain frequency components across much of the spatial frequency spectrum, and the spatial frequencies of the lines and band overlapped. These difficulties with band extraction can be eliminated with better spectrometer resolution.

Specific types of emissions (line, band, and continuum) typically are expressed over a range of spatial frequencies rather than at a single spatial frequency. Therefore, frequency components of the specific types of emissions may overlap. If the magnitudes of these overlapping components are large, filtering will cause corruption in the extracted phenomena.

Poor spectrometer resolution causes difficulties with spectral analysis. Poor resolution prevents isolation of closely spaced spectral lines, causes the lines to appear much broader than they actually are, and results in the inability to separate the spatial frequency components of line and band emissions. It was determined that the required resolution for SSME plume spectral monitoring is 0.03 nm

For the spectra analyzed in this paper, spectrometer resolution was not adequate to separate closely spaced lines or separate the spatial frequency components of the lines and bands. Therefore, the cutoff spatial frequencies for the filters were determined by trial and error. the cutoff frequencies were: 0.025 cycles/nm for the low pass filter, 0.025 cycles/nm for the high pass filter, and 0.010 through 0.210 cycles/nm for the band pass filter.

As an example of digital filtering implementation, the 100 spectral scans recorded from engine number 2031 during test number 904-047 on August 11, 1989 at the NASA Stennis Space Center were analyzed using the techniques discussed in this paper. This analysis revealed no anomalous conditions in the engine. Irradiances of the spectral lines corresponding to metallic species were constant throughout the test with respect to power level, indicating normal engine wear. Similar results were obtained from the standard post firing engine analysis.

References

1. Cikanek, H.A., et al., "Space Shuttle Main Engine Plume Spectral Monitoring - Preliminary Results," AIAA Paper 87-1792, June 1987.

2. Linbaugh, C.C., et al., "Analysis of SSME Plume Images During Ground Testing," 1987 JANNAF Propulsion Meeting. Vol. 5, D.S. Eggelston and K.L. Strange, eds., CPIA-PUBL-480-VOL-5, Chemical Propulsion Information Agency, Laurel, MD, 1987, pp. 215-223 (Avail. NTIS, AD-B137172).

3. Powers, W.T., "Rocket Plume Spectrometry: A System Permitting Engine Condition Monitoring, as Applied to the Technology Test Bed Engine," Structural Integrity and Durability of Reusable Space Propulsion Systems, NASA CP-10030, 1989, pp. 127-135.

4. Powers, W.T. and Cikanek, H.A., "Analysis of UV-VIS Spectral Radiation From SSME Plume," Advanced Earth to Orbit Propulsion Technology 1988, Vol. 2, R.J. Richmond and S.T. Wu, eds., NASA CP-3012-VOL-2, 1988, pp. 595-611.

5. Chenevert, D.J., "Combined Spectral and Video Monitoring of SSME Plumes," NASA John C. Stennis Space Center, Bay Saint Louis, MS, unpublished research.

6. Swaminathan, P.K., et al., "Calculation of Kinetic Data for Processes Leading to UV Signatures," AFOSR-89-0395TR, 1989 (Avail. NTIS, AD-A206656).

7. Young, S.J., "Inversion of Plume Radiance and Absorptance Data for Temperature and Concentration," AFRPL-TR-78-60, 1978 (Avail. NTIS, AD-A068437).

8. Buchele, D.R., "Computer Program for Calculation of a Gas Temperature Profile by Infrared Emission: Absorption Spectroscopy," NASA-TM-73848, 1977.

9. Reader, J., et al., "Wavelengths and Transition Probabilities for Atoms and Atomic Ions," NSRDS-NBS-68, National Standard Reference Data System, National Bureau of Standards, 1980 (Avail. U.S.G.P.O., PB81-206120).

10. Pearse, R.W.B. and Gaydon, A.G., The Identification of Molecular Spectra, 3rd ed., Wiley, New York, 1963.

11. Alkemade, C.J., et al., Metal Vapours in Flames, Pergamon Press, New York, 1982.

12. Ingle, J.D. and Crouch, S.R., Spectrochemical Analysis, Prentice Hall, Englewood Cliffs, NJ, 1988.

13. Gonzalez, R.C. and Wintz, P.A., Digital Image Processing, Addison-Wesley, Reading, MA, 1977.

14. Press, W.H., et al., Numerical Recipes: The Art of Scientific Computing, Cambridge University Press, New York, 1986.

15. Marple, S.L., Jr., Digital Spectral Analysis - with Applications, Prentice-Hall, Englewood Cliffs, NJ, 1987.

16. Cooley, J.W., Lewis, P.A.W., and Welch, P.D.,"The Fast Fourier Transform and its Applications," IEEE Transactions on Education, Vol. E-12, No. 1, Mar. 1969, pp. 27-34.

TABLE 1. Spectral Features in SSME Plume

Species	Wavelengths (nm)	Source
Al	308.22/309.27/394.40/396.15	Present in Structural Materials
Ca	422.67/443.50/445.48/445.58/534.95/558.88 559.45/585.75/610.27/612.22/616.22/616.95 643.91/644.98/646.26/647.17/649.38/649.97 671.77/714.81/720.22/732.62	Bearing Cages
C	477.18/493.21/505.22/538.03/600.11/600.60 601.32/601.48/658.76/711.32/711.52/711.70 786.09/805.86	Present in Structural Materials
Cr	357.87/359.35/360.53/396.34/425.44/427.48 428.97/434.45/435.18/520.45/520.60/520.84	Present in Structural Materials
Co	340.51/341.23/344.36/345.35/346.28/346.58 347.40/350.23/350.63/352.69/352.98/356.94 358.72/384.55/387.31/389.41/399.53	Present in Structural Materials
Cu	301.08/303.61/306.34/310.86/324.75/327.40 330.80/353.04/406.26/465.11/510.55/515.32 521.82/570.02/578.21/793.31/809.26	MCC Liner, PB Baffles, LPOTP
Au	242.80/267.60/274.83/312.28/406.51/460.75	Brazing Materials
H	486.13/656.27/656.29	Propellant
Fe	344.06/358.12/371.99/373.49/373.71/374.56 374.83/374.95/385.99/388.63/404.58/438.35	Present in Structural Materials
Li	323.27/391.53/413.26/427.31/610.36/670.78	Dry Film Lubricant
Mn	403.08/403.31/403.45/404.14	Valves, Flex Joints
Mo	313.26/317.04/379.83/386.41/390.30/550.65	FPB/OPB Faceplates, Seals
Ni	341.48/344.63/345.85/346.17/349.30/351.51 352.45/356.64/361.94	Present in Structural Materials
N	496.40/575.25/582.95/646.84/648.17/648.27 648.38/648.48/740.62/742.36/744.23/746.83 818.49/818.80/821.07/821.63/822.31/824.24	Present in Atmosphere
O	615.68/615.82/700.22/725.45/777.19/777.42 777.54	Propellant
K	404.41/404.72/578.24/580.18/581.22/583.19 691.11/693.88/766.50/769.90	Present in Propellants

TABLE 1. Continued

Species	Wavelengths (nm)	Source
Ag	328.07/338.29/520.91/546.55	MCC, PB Baffles, LPOTP, Brazing
Na	330.23/330.30/449.42/449.77/568.82/589.00 589.59	Present in Propellants
Sr	460.73/496.23/548.08/640.85/650.40/707.01	Present in Structural Materials
Ta	304.96/306.92/310.33/318.10/331.12/331.88 337.15/360.74/362.66/364.21	Present in Structural Materials
Ti	319.20/319.99/334.19/335.46/337.14/363.55 364.27/365.35/374.11/375.29/394.87/395.63 395.82/398.18/398.98/399.86/430.11/430.59 453.32/453.47/498.17/499.11/499.95/500.72 501.42	Present in Structural Materials
W	400.88/407.44/429.46/430.21	LOX Posts, Turbines
CaO	547 - 556	
CaOH	553 - 557/620 - 630	
CrO	639 -645	
CuH	425 - 435	
CuO	604 - 611/614 - 620	
CuOH	535 - 555/615 - 625	
FeO	560 - 570/580 - 600/622 - 635/810 - 830	
FeOH	353 - 358/363 - 368	
MnH	474 - 484/558 - 586	
MnOH	350 -400	
OH	305 - 315	Combustion
SrOH	600 - 610/679 - 685	
TiO	455 - 495/515 - 525/545 - 555/610 - 640	
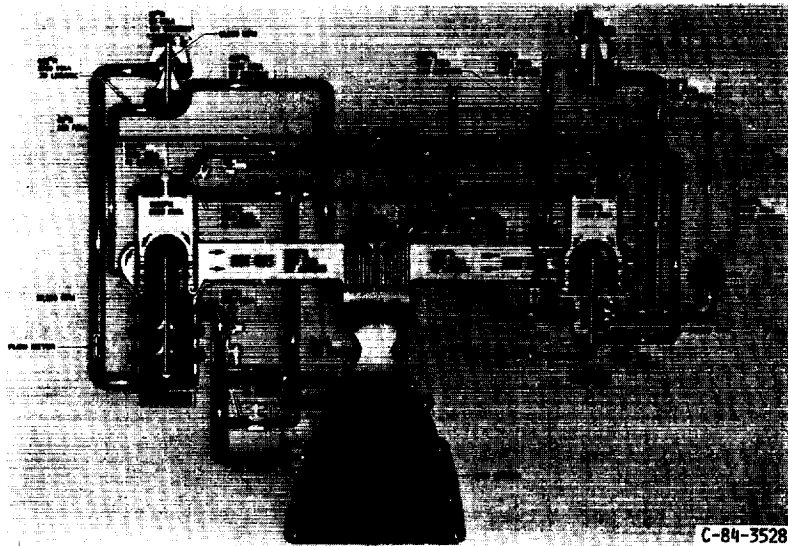
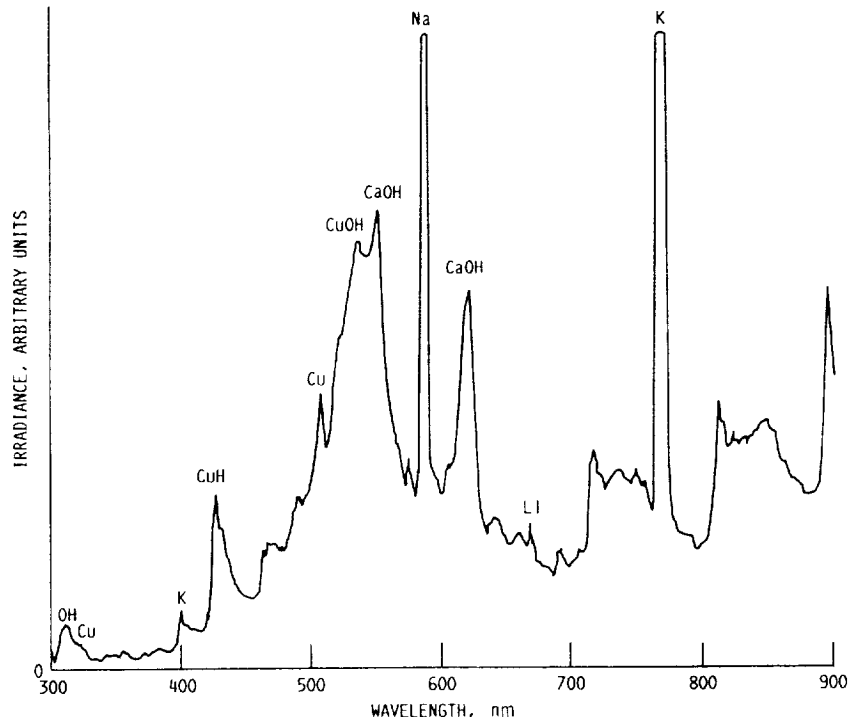FIGURE 1. - SSME PROPELLANT FLOW PATHS.

FIGURE 2. - TYPICAL SPECTRAL SIGNATURE FROM SSME.

SSME PLUME SPECTRA
25 MARCH 1988
A-3 TEST #750-314
ENGINE 0208

EXPOSURE TIME: 0.10 SECONDS/SUBFILE
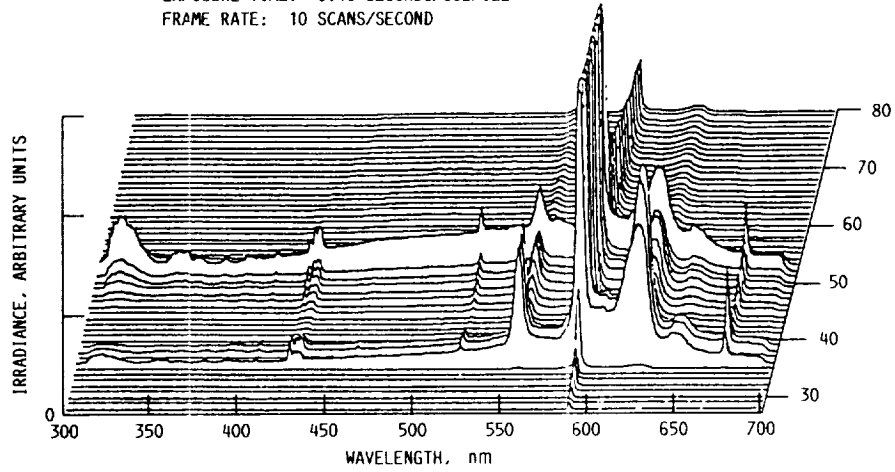FRAME RATE: 10 SCANS/SECOND

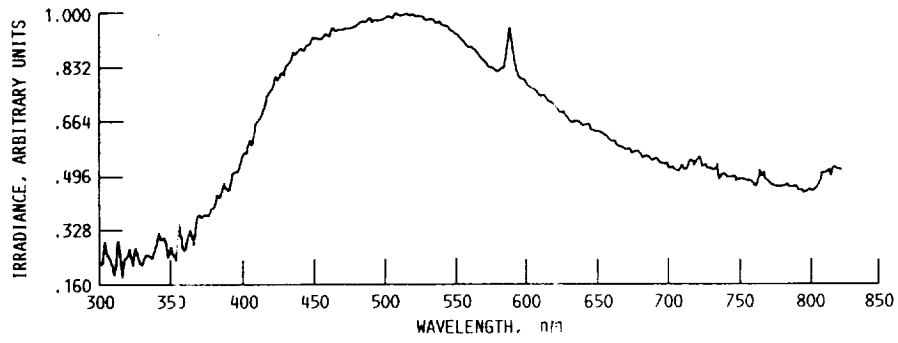FIGURE 3. - TIME SERIES OF EMISSION SPECTRA FROM SSME.
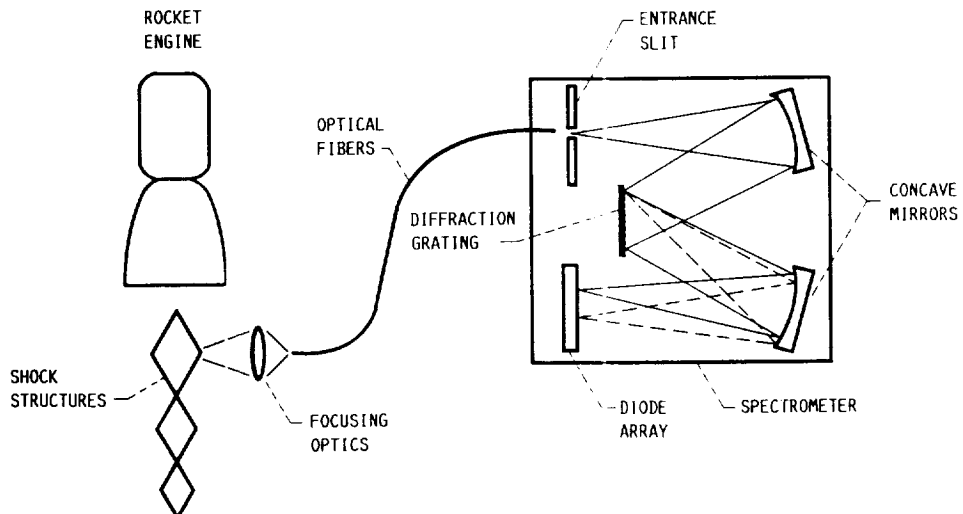
FIGURE 4. - SSME EMISSION SPECTRUM.

FIGURE 5. - EMISSION SPECTROSCOPY OF ROCKET ENGINE EXHAUST PLUME.
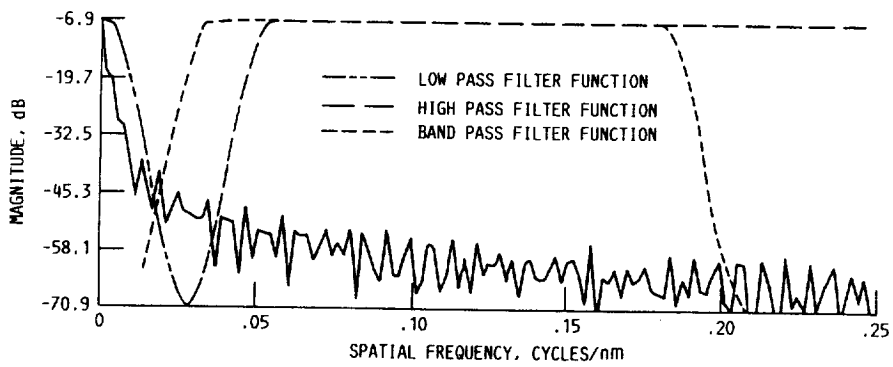
FIGURE 6. - FOURRIER TRANSFORM OF SSME EMISSION SPECTRUM. DASHED LINES INDICATE
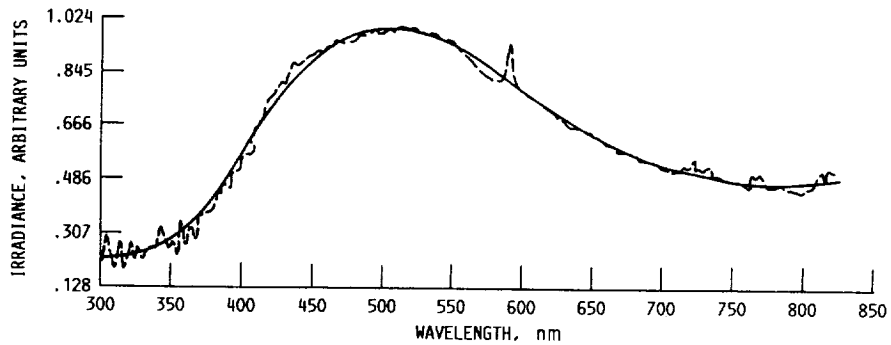THE VARIOUS FILTER FUNCTIONS.

FIGURE 7. - EMISSION SPECTRUM AFTER LOW PASS FILTERING. THE SOLID LINE IS THE FIL-
TERED SPECTRUM, AND THE DASHED LINE IS THE UNFILTERED SPECTRUM.
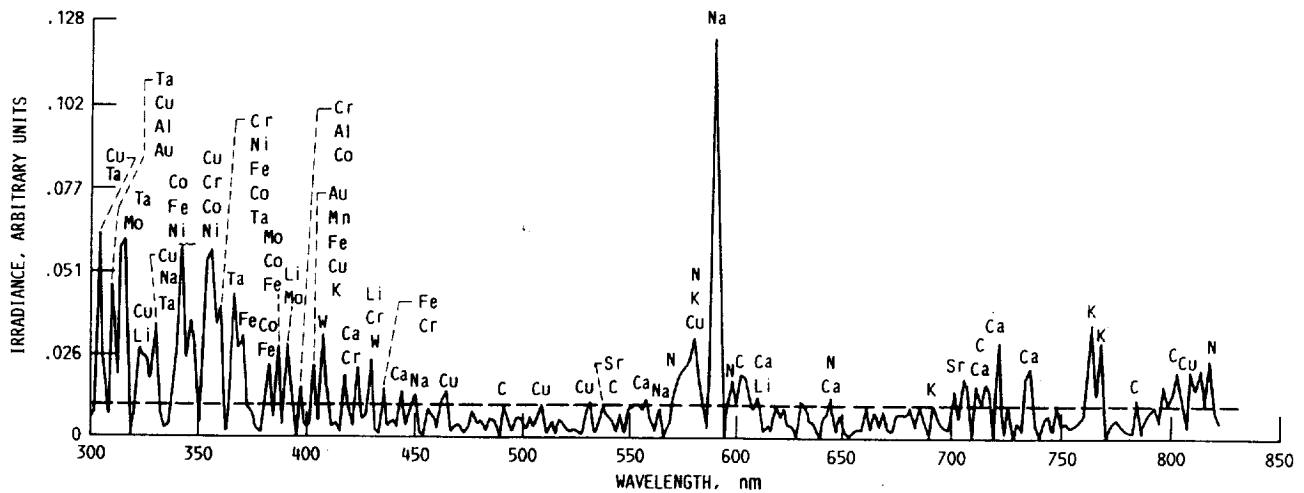

FIGURE 8. - EMISSION SPECTRUM AFTER HIGH PASS FILTERING. DASHED LINE INDICATES THE NOISE FLOOR. POOR SPECTROMETER RESOLU-
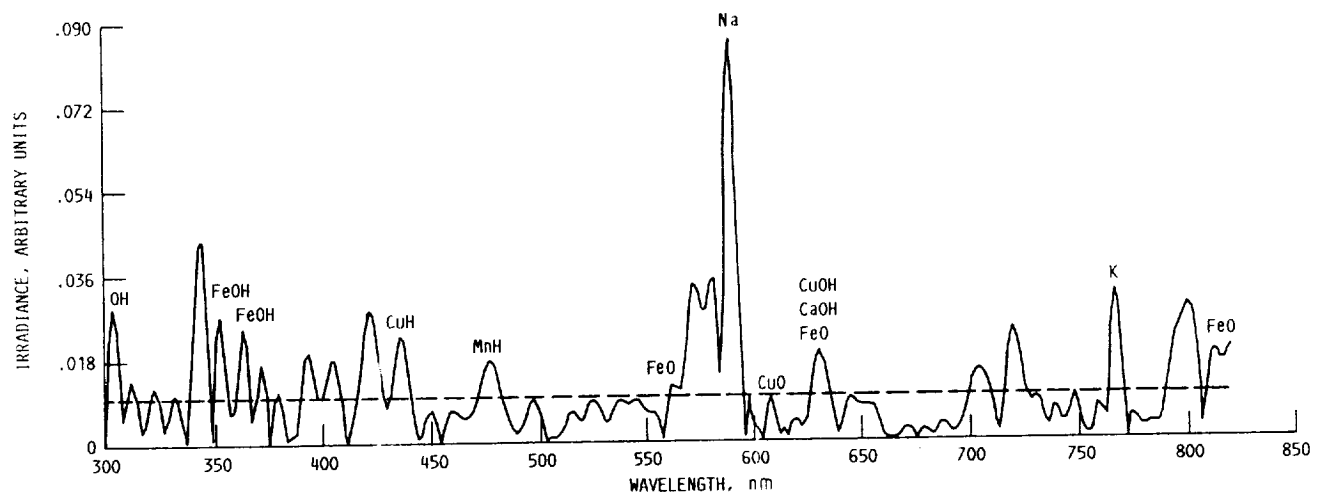TION DID NOT ENABLE SEPARATION OF CLOSELY SPACED LINES; THEREFORE SOME LINES HAVE MULTIPLE LABLES.

FIGURE 9. - EMISSION SPECTRUM AFTER BAND PASS FILTERING. THE DASHED LINE INDICATES THE NOISE FLOOR.

NASA
National Aeronautics and Space Administration

Report Documentation Page

1. Report No. NASA TM-103135 AIAA-90-1994	2. Government Accession No.	3. Recipient's Catalog No.

4. Title and Subtitle	5. Report Date
Digital Filtering of Plume Emission Spectra	
	6. Performing Organization Code

7. Author(s)	8. Performing Organization Report No.
George C. Madzsar	E-5478
	10. Work Unit No. 590-21-41

9. Performing Organization Name and Address	11. Contract or Grant No.
National Aeronautics and Space Administration Lewis Research Center Cleveland, Ohio 44135-3191	
	13. Type of Report and Period Covered

12. Sponsoring Agency Name and Address	Technical Memorandum
National Aeronautics and Space Administration Washington, D.C. 20546-0001	14. Sponsoring Agency Code

15. Supplementary Notes

Prepared for the 26th Joint Propulsion Conference cosponsored by the AIAA, ASME, SAE, and ASEE, Orlando, Florida, July 16–18, 1990.

16. Abstract

Fourier transformation and digital filtering techniques were used to separate the superpositioned spectral phenomena observed in the exhaust plumes of liquid propellant rocket engines. Space shuttle main engine (SSME) spectral data were used to show that extraction of spectral lines in the spatial frequency domain does not introduce error, and extraction of the background continuum introduces only minimal error. Error introduced during band extraction could not be quantified due to poor spectrometer resolution. Based on the atomic and molecular species found in the SSME plume, it was determined that spectrometer resolution must be 0.03 nm for SSME plume spectral monitoring.

17. Key Words (Suggested by Author(s))	18. Distribution Statement
Plume; Plume emission; Rocket engine; Diagnostics; Health monitoring; Fourier analysis; Digital filtering; Filtering	Unclassified – Unlimited Subject Category

19. Security Classif. (of this report)	20. Security Classif. (of this page)	21. No. of pages	22. Price*
Unclassified	Unclassified	12	A03